Bone Regeneration with BMP-2 Gene-modified Mesenchymal Stem Cells Seeded on Nano-hydroxyapatite/Collagen/ Poly(L-Lactic Acid) Scaffolds

JIN-LEI DONG, LIAN-XIN LI, WEI-DONG MU, YONG-HUI WANG AND DONG-SHENG ZHOU*
Department of Orthopedics, Provincial Hospital Affiliated to Shandong University, Jinan 250021, People's Republic of China

WEI HAO
Department of Spinal Cord Injury, General Hospital of Ji'nan Military Area, Jinan 250031, People's Republic of China

DE-BO ZOU
Department of Orthopedics, Qianfoshan Hospital Affiliated to Shandong University, Jinan 250014, People's Republic of China

KUN HU
Institute of Nuclear and New Energy Technology Tsinghua University, Beijing 100084, People's Republic of China

JI LI
Department of Orthopedics, Jinan Fourth Hospital Jinan 250031, People's Republic of China

FU-ZHAI CUI*
State Key Laboratory of New Ceramics and Fine Processing Department of Materials Science and Engineering, Tsinghua University Beijing 100084, People's Republic of China

*Authors to whom correspondence should be addressed.
E-mail: orthodjl@yahoo.com.cn; cuifz@mail.tsinghua.edu.cn
Figures 2, 3 and 8 appear in color online: http://jbc.sagepub.com

0883-9115/10/06 0547–20 $10.00/0 DOI: 10.1177/0883911510380436

ABSTRACT: In this study, the capacity of bone morphogenetic protein 2 (BMP-2) gene-transfected bone marrow-derived mesenchymal stem cells (MSCs) in combination with nano-hydroxyapatite/collagen/poly(L-lactic acid) (nHAC/PLA) to improve the repair of bone defects in rabbit was explored. MSCs from New Zealand White rabbits were cultured and injected with pIRES2-EGFP-hBMP-2 or pIRES2-EGFP by electroporation. After the transfer efficiency was determined through the expression of EGFP, the MSCs were seeded on scaffolds to generate an *in vitro* 3D cell/scaffold construct. The adhesion and proliferation of the MSCs cultured in the scaffold was assessed by SEM. The cellular constructs obtained were allografted into the 15 mm critical-sized segmental bone defects in the radius of New Zealand White rabbits for 12 weeks. The bone regeneration was assessed by radiographical and histological analyses. *In vitro*, nHAC/PLA facilitated MSC adhesion and proliferation on the scaffold, and gene transfer efficiency reached a maximum of $35.5 \pm 3.8\%$. *In vivo*, the implantation of BMP-2 transfected MSCs/nHAC/PLA construct significantly enhanced the formation of new bone in the segmental defect, compared to the control groups. This novel 3D BMP-2 transfected MSCs/nHAC/PLA construct has the potential for bone repair by genetic tissue engineering approach.

KEY WORDS: tissue engineering, genetic tissue engineering, mesenchymal stem cells, BMP-2, nHAC/PLA scaffold, osteogenic activity, allograft, segmental bone defect, bone regeneration, gene transfer.

INTRODUCTION

A challenge for orthopedic surgeons remains with respect to the repair of large bone defects caused by trauma, tumors, and severe inflammation [1,2]. Patients with large lesions never heal spontaneously and the damaged sites have limited potential to totally recover. Autogenous osteochondral grafts and allografts are the most common procedures. These, however, have innate problems such as autogenic bone availability and donor-site morbidity [3,4], and are limited in usage due to possible immunological rejection and transmission of pathogens [5,6]. Currently, efforts to provide genetically engineered tissue as an alternative to the traditional treatment that can meet the needs of an individual patient are being pursued [7,8].

Typically, tissue-engineered bone possesses three essential components: (1) a cell source; (2) appropriate osteoinductive factors; and (3) an appropriately designed scaffold [9]. In fact, using the patient's bone marrow-derived mesenchymal stem cells (MSCs) may be an ideal cell source for tissue-engineered bone. These are easily obtained and potentially can be used to develop bone, muscle, cartilage, adipose, and fibrous tissues [10–13]. In many reports, the ultimate fate of

undifferentiated stem cells is determined by the local environment in which it is located [7]. Exogenous bone morphogenetic proteins (BMPs) are known to stimulate osteoblastic differentiation [14]. Among the BMP subtypes, BMP-2, in particular, possesses high bone induction activity and stimulatory effects on MSCs to differentiate into osteoblasts [15]. To maximize the osteogenic capacity of MSCs, the application of exogenous BMP-2 has frequently been used to promote the osteogenic differentiation of MSCs and *in vitro* BMP-2 gene therapy [16–18]. For example, autologous MSCs, genetically modified to express BMP-2 via *in vitro*, enhance bone formation [19,20].

To construct a genetic tissue-engineered product, the selection of an appropriate scaffold is critical [21]. Scaffolds such as poly(L-lysine)-coated polylactide (PLA) [22], poly(DL-lactic-co-glycolic) acid (PLGA), alginates [23], and β-tricalcium phosphate (β-TCP) [24] have been used. A 3D porous polymeric matrix enhances bone regeneration and facilitates progenitor cell adhesion, proliferation, and differentiation [21,25–27]. Nano-hydroxyapatite/collagen/poly(L-lactic acid) (nHAC/PLA), as a biodegradable 3D porous scaffold, appears to be a good candidate as a carrier for gene-modified cells. The nHAC/PLA developed by biomimetic synthesis exhibits features of natural bone both in the main composition and hierarchical microstructure [28].

In previous studies, we demonstrated that biodegradable 3D porous nHAC/PLA scaffolds are capable of supporting osteoblastic cell attachment and proliferation throughout the scaffold while maintaining the osteoblastic phenotype [29]. Furthermore, the biocompatibility and osteoconductivity of nHAC/PLA composite have been examined *in vivo* [30,31]. In this study, we constructed a mammalian plasmid vector of pIRES2-EGFP-hBMP-2 and transferred the BMP-2 gene into MSCs by electroporation. These gene-modified MSCs were then seeded onto nHAC/PLA scaffolds to develop cell/scaffold construct. The *in vitro* attachment and the growth of BMP-2 transfected cells in the scaffold were investigated. *In vivo*, we observed the repair of segmental bone defects after the implantation of cell/scaffold construct.

MATERIALS AND METHODS

Plasmid Construction

The recombinant eukaryotic expression plasmid pIRES2-EGFP-hBMP-2 was constructed as described previously [32]. Briefly, the human BMP-2 cDNA was cloned and sequenced from human

osteosarcoma tissue. The PCR product was then ligated into a pMD18-T simple vector (Takara, Japan) for DNA sequencing, and was then further subcloned into a mammalian expression vector, pIRES2-EGFP (Clontech, CA). The constructed pIRES2-EGFP-hBMP-2 plasmid was confirmed by Bgl II/Sal I enzyme digestion.

Isolation and Culture of MSCs

MSCs were obtained from 3-month-old New Zealand White rabbits. Bone marrow was aspirated from the rabbit tibia and femur. After being washed twice with sterilized phosphate buffered saline (PBS) to exclude any fatty tissue and blood clots, the bone marrow was gently layered onto Percoll lymphocyte separation liquid (density 1.073 g/mL; Gibco, USA) and centrifuged at 2000 r/min for 15 min. The nucleated cells were collected from the middle layer, washed twice with PBS, and resuspended in 10 mL of low-glucose Dulbecco's modified Eagle's medium (DMEM, Gibco, USA) containing 10% fetal bovine serum (FBS; Gibco, USA) and 1% antibiotics. The cells were cultured in a 50 mL flask at 37°C in a humidified atmosphere with 5% CO_2. The medium was changed after 5 days to remove cells that had not adhered to the culture flask. Thereafter, the medium was completely replaced every other day. After 12–16 days, the adherent cells were near confluence in 75 cm^2, at which time the cells were digested in 0.25% trypsin and subcultured. The MSCs obtained were passaged and subsequently used for gene transfection.

BMP-2 Gene Transfection into MSCs

The second-passage MSCs were transfected using the electroporation. Briefly, 15 μg of pIRES2-EGFP-hBMP-2 plasmid DNA was diluted to 2×10^5 of second-passage MSCs in 0.2 mL of sterilized PBS. Then, they were transferred to 4 mm cuvettes and electroporated at 500 V/30 μs using a Square Wave Electroporation System, ECM 830 (BTX). Before and after transfection, the cells were incubated at 4°C for 5 min (mixture of ice and water); the transfected cells were then plated on 6 cm dishes with growth medium at 37°C. The medium was changed every 24 h. MSCs were also transfected with pIRES2-EGFP empty vectors (Mock) as control. Using a fluorescence microscope (Leica, DMIRE-2, Germany) [33], the gene transfer efficiency was assayed as a function of EGFP expression by scoring the percentage of EGFP-positive cells among all the cells present in 10 randomly selected 20 × fields.

Reverse Transcriptase Polymerase Chain Reaction Analysis

Total RNA was isolated from MSCs transfected by BMP-2 or mock plasmid, or untransfected using Trizol reagent (Invitrogen, USA) according to the manufacturer's protocol. Total RNA (2.5 μg) was reverse transcribed into cDNA in a 20 μL reverse transcription system (Fementas, Lithuan) according to the manufacturer's instructions. The cDNA samples were amplified and the specific primers were displayed as follows: hBMP-2: sense, TCAAGCCAAACACAAACAGC; and antisense, ACGTCTGAACAATGGCATGA (product size, 200 bp); ß-actin: sense, TGTGCCCATCTACGAGCGGTATGC; antisense, GGTACATGGTGCC GCCAGACA (product size, 439 bp). PCR products were separated on 1% agarose gels and visualized by ethidium bromide staining.

Quantitative Measurement of Alkaline Phosphatase Activity

To analyze the osteogenic differentiation of MSCs, intracellular alkaline phosphatase (ALP) activity was determined. The level of ALP activity was measured on days 1, 7, and 14 after gene transfer. The cells were rinsed twice with sterilized PBS followed by lysis with NP-40 buffer. The ALPase activity of cell lysates was determined by measuring the release of *p*-nitrophenol from *p*-nitrophenyl phosphate (Sigma) as substrate. The release of *p*-nitrophenol was monitored by measuring the optical density at 405 nm. The optical densities were compared to a *p*-nitrophenol standard (Sigma). The enzyme activity was expressed as nanomoles of *p*-nitrophenol/h/mg of total cellular protein.

Fabrication of nHAC/PLA Scaffold

The nHAC/PLA scaffold was synthesized as previously reported [34]. Type I collagen (CELLON Company, USA) was stirred at 4°C with 0.67 g of collagen/L to obtain a solution. To this, solutions of $CaCl_2$ and H_3PO_4 (Ca/P = 1.66) were added separately dropwise and the pH was adjusted to 7.4 by adding 0.75 M NaOH. The nHAC deposition was obtained 48 h later by centrifugation and freeze-drying. PLA (100,000 Mw) was dissolved in 1,4-dioxane to form a final 8% (w/v) solution and stirred for 4–6 h. To this solution, nHAC powder was added. The solution was ultrasonicated, poured into a mold, and cooled at −20°C overnight. The frozen composites were lyophilized to remove the 1,4-dioxane. Then, the porous composite scaffold obtained was cut into small disks with 8 mm in diameter and 2 mm in thick for *in vitro* cell cultures ($15 \times 5 \times 3\,mm^3$ for animal experiment).

Cell Seeding

For cell culture, the nHAC/PLA scaffolds were sterilized by γ-ray irradiation (2.5 Mrad), rinsed thoroughly with sterilized PBS, and immersed in the culture medium overnight. The slices were placed in 48-well tissue culture clusters (Costar, USA) and each scaffold was seeded with 5×10^5 BMP-2 transfected MSCs or mock-transfected MSCs suspended in 100 μL of complete medium. After incubating at 37°C in a humidified atmosphere with 5% CO_2 for 3 h, an additional 900 μL of culture medium was added to each well. The medium was changed every 2 days.

Scanning Electron Microscopy Examination

The adhesion and growth of MSCs on the scaffolds was observed by scanning electron microscopy (SEM) after 2 and 24 h cell seeding. All the cell/scaffold constructs were rinsed twice with sterilized PBS to remove the nonadherent cells, fixed in 2.5% glutaraldehyde for 12 h at 4°C, then rinsed three times with PBS, and dehydrated, consecutively, in 30%, 50%, 70%, 75%, 80%, 90%, 95%, and 100% ethanol for 10 min each. The samples were then critical point dried, coated with a thin layer of gold–palladium through sputtering under an argon atmosphere prior to SEM observation (Hitachi S-520, Japan).

Surgical Procedure

Twenty healthy New Zealand White rabbits of both sexes weighting about 3.0 kg were used as experimental animals. All surgical procedures followed protocols were approved by the Animal Care Committee of the Medical School of Shandong University, and were based on a well-established rabbit, critical-sized segmental bone defect model.

The rabbits were divided into four groups ($n = 5$). Group A for the implantation of nHAC/PLA scaffolds combined with BMP-2 transfected MSCs, Group B for nHAC/PLA scaffolds combined with mock-transfected MSCs, Group C for just nHAC/PLA scaffolds, and Group D for blank control. Briefly, rabbits were anesthetized by intravenous injection of pentobarbital sodium (25 mg/kg). Both the radii of each animal were operated upon. A 4 cm longitudinal incision was made in the shaved skin along the radius with a sterile blade. Muscles were dissected open to expose the diaphyseal portion of the radius. After excision of the periosteum, a 15 mm long section of the diaphysis was removed using a cutting saw under constant cooling with saline. A $15 \times 3 \times 3\,mm^3$ sized scaffold or cell/scaffold construct was inserted into the defect.

For cell/scaffold construct, each nHAC/PLA scaffold ($15 \times 3 \times 3\,mm^3$) was seeded with 5×10^6 cells as described in the *in vitro* study. One day after cell seeding, the cell/scaffold construct was implanted in the defect and the rabbits were allowed to move freely in their cages.

Radiographic and Histological Analyses

Rabbits from each group were sacrificed at 8 and 12 weeks post-operation. The whole radius was excised and examined using X-ray radiography at certain implantation period. For histological studies, the radius was fixed in 10% formalin neutral buffer solution at pH 7.4 for 2 days at 4°C and then decalcified with 10% HCI and 0.1% ethylene diamine tetra-acetic acid (EDTA) at 4°C for another 2 days. The specimens were then dehydrated using graded ethanols and embedded in paraffin. Tissue blocks were then sectioned with at thickness of 5 μm in thickness, stained with hematoxylin and eosin (HE), and observed by light microscope (Olympus, Japan).

Statistical Analysis

All quantitative data were expressed as means ± standard deviation (SD). Statistical analysis was assessed using SPSS (v13.0). A Student's *t*-test (assuming equal variances) was performed to determine the statistical significance between the experimental groups. A value of $p < 0.01$ was accepted to be statistically significant.

RESULTS

Plasmid Construction and MSC Culture

The hBMP-2 gene was amplified from human osteosarcoma tissue (Figure 1(a)) and the sequences of hBMP-2 cDNA were confirmed by DNA sequencing (GenBank NM-001200). The amplified hBMP-2 gene was inserted into the pIRES2-EGFP vector to construct the pIRES2-EGFP-hBMP-2 mammalian expression vector. This process was confirmed by double enzymatic digestion with Bgl II and Sal I. The expected bands were observed following gel electrophoresis (Figure 1(b)).

The nucleated cells were isolated by density gradient centrifugation using Percoll (1.073 g/mL) and plated in complete medium. The initial adherent cells grew into spindle-like or stellate-shaped cells, which

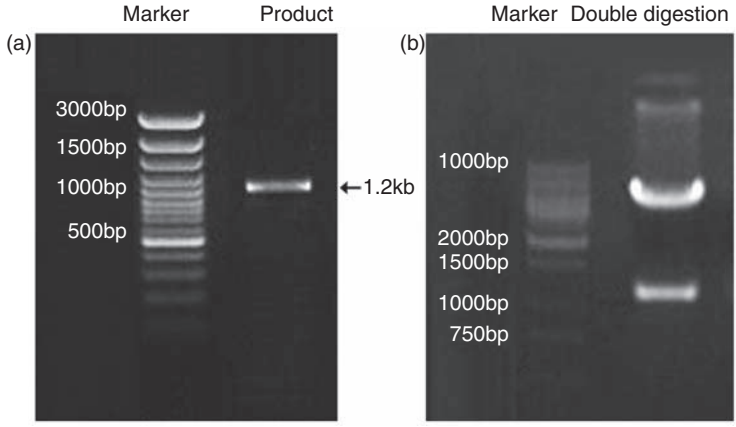

Figure 1. (a) The 1.2-kb hBMP-2 gene was amplified from human osteosarcoma tissue. (b) Construct of pIRES2-EGFP-hBMP-2 was confirmed by double digestion with Bgl II and Sal I.

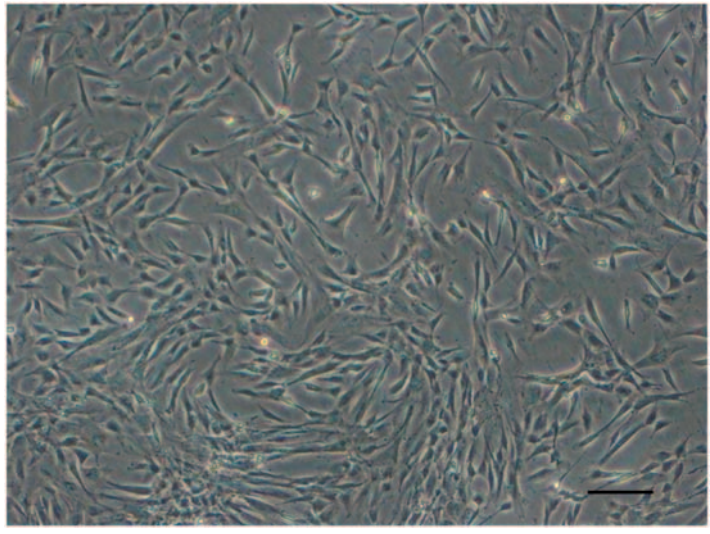

Figure 2. Rabbit MSCs of second passage with a fibroblast-like shape (bar = 100 μm).

developed into visible colonies 3–5 days after initial plating. After 2–3 days, the cells began to proliferate rapidly, reaching confluence on the 12th to 16th day. The nonadherent hematopoietic cells were discarded by changing medium. Following further passages the MSCs proliferated uniformly. The cells maintained a homogeneous fibroblast-like morphology with a spindle-shaped appearance (Figure 2).

BMP-2 Expression in BMP-2 Transfected MSCs

The quantification of gene transfer efficiency in the modified MSCs was determined by assessing the number of EGFP-expressing cells under inverted fluorescent microscope. After electroporating at 500 V and 30 μs, a transfer efficiency of $35.5 \pm 3.8\%$ was achieved (Figure 3). The remaining experiments were carried out based on those parameters. EGFP expression was initially detected 8 h after gene transfer and climaxed between 48 and 72 h afterwards.

Reverse transcriptase polymerase chain reaction (RT-PCR) was an easy and efficient way to detect gene expression in RNA. The mRNA expression of hBMP-2 among MSCs was confirmed 1 day after electroporation. As shown in Figure 4, the BMP-2 transfected MSCs had both the 200-bp-specific amplification bands of hBMP-2 and the 439-bp-specific amplification band of β-actin. Mock-transfected MSCs and untransfected MSCs had no 200-bp-specific amplification bands, but did have the 439-bp-specific amplification band of β-actin.

ALP Activity

ALP is one of the early markers of osteoblasts and it increases as the bone formation progresses, particularly, during mineralization. ALP activity was determined to quantify the *in vitro* osteogenic activity of the genetically modified MSCs. Comparing the ALP activity of BMP-2 transfected MSCs and mock-transfected MSCs, as shown in Figure 5, there was no statistical difference on the 1-day time period ($p > 0.01$). After 7 and 14 days of gene transfer, the ALP expression of BMP-2 transfected MSCs was markedly higher than the control ($p < 0.01$). These results indicated that BMP-2 gene therapy promoted MSC differentiation into osteoblastic cells.

Scanning Electron Microscopy

By SEM observation, the BMP-2 transfected MSCs started to attach and grow from 2 h after cells seeding on the scaffolds. Representative SEM images in Figure 6(c) show that cell attachment to the scaffold after 2 h of culture had occurred; the cells on the nHAC/PLA scaffold surfaces exhibited a globular shape with numerous microspikes and extended filopodia that attached to the scaffolds. After 1 day, a confluent layer of cells had proliferated in the scaffold. The BMP-2 transfected MSCs exhibited a highly flattened shape and attached to the pore wall of the scaffold with their pseudopodia with partial bridging over some

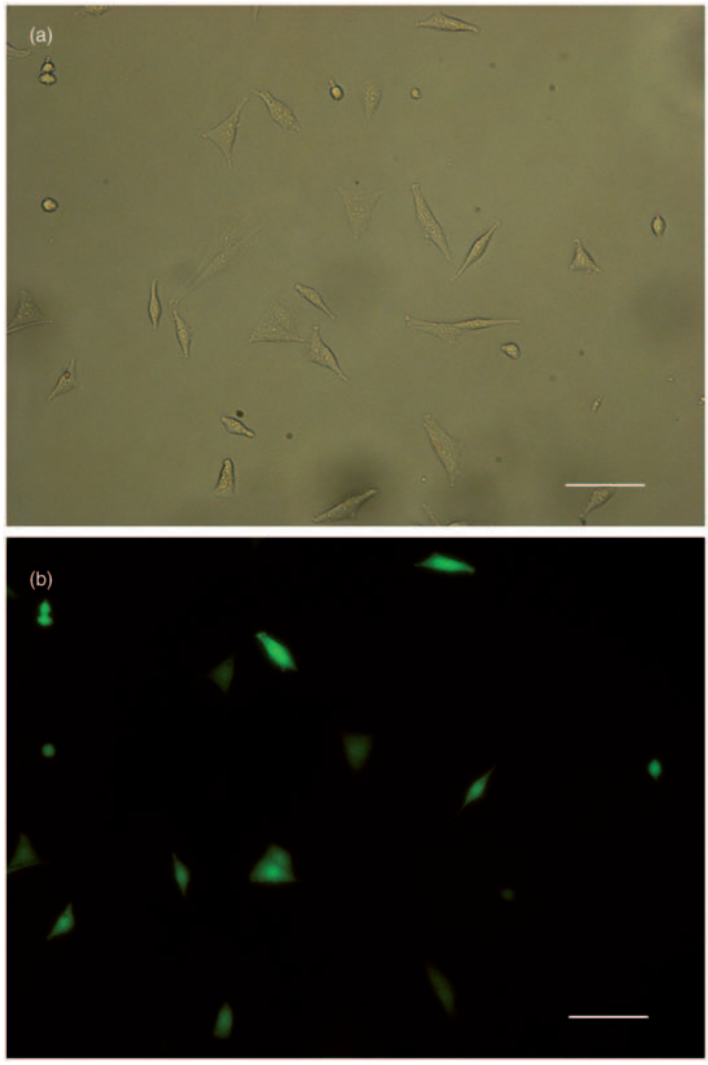

Figure 3. Quantification of gene transfer efficiency into the MSCs was determined by EGFP expression using fluorescent microscope 3 days after gene transfection (bar = 100 μm): (a) photograph of MSCs transfected with pIRES2-EGFP-hBMP-2 (phase contrast microscope); (b) the field in the previous photograph was taken with fluorescent microscope.

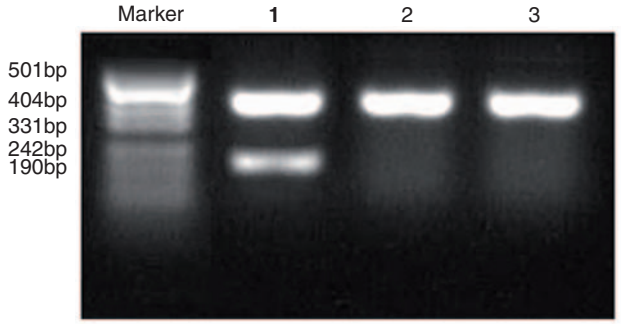

Figure 4. mRNA expression of hBMP-2 detected by RT-PCR. Lane 1, BMP-2 transfected MSCs; lane 2, mock-transfected MSCs; lane 3, untransfeced cells.

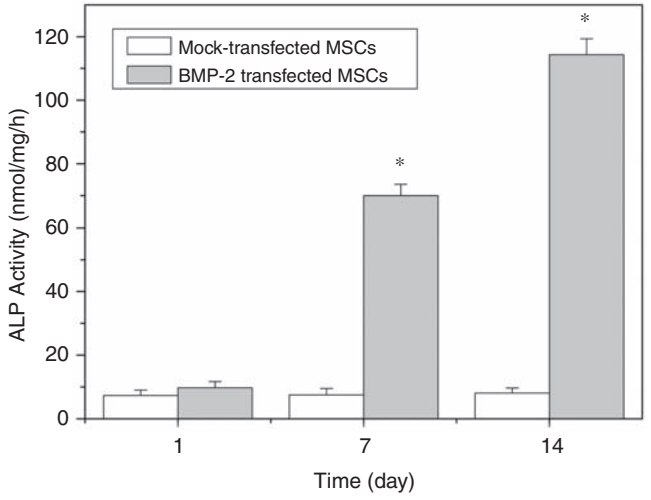

Figure 5. ALP activity of BMP-2 transfected MSCs and mock-transfected MSCs. Data were displayed as means $\pm$ SD ($n = 3$, $^*p < 0.01$).

pores (Figure 6(d)). In addition, the acellular nHAC/PLA scaffolds are observable in Figure 6(a) and (b).

Radiographic Examination

All the rabbits survived to the follow-up 12-week period with no signs of inflammation or infection. Ossification bridging at both ends of the

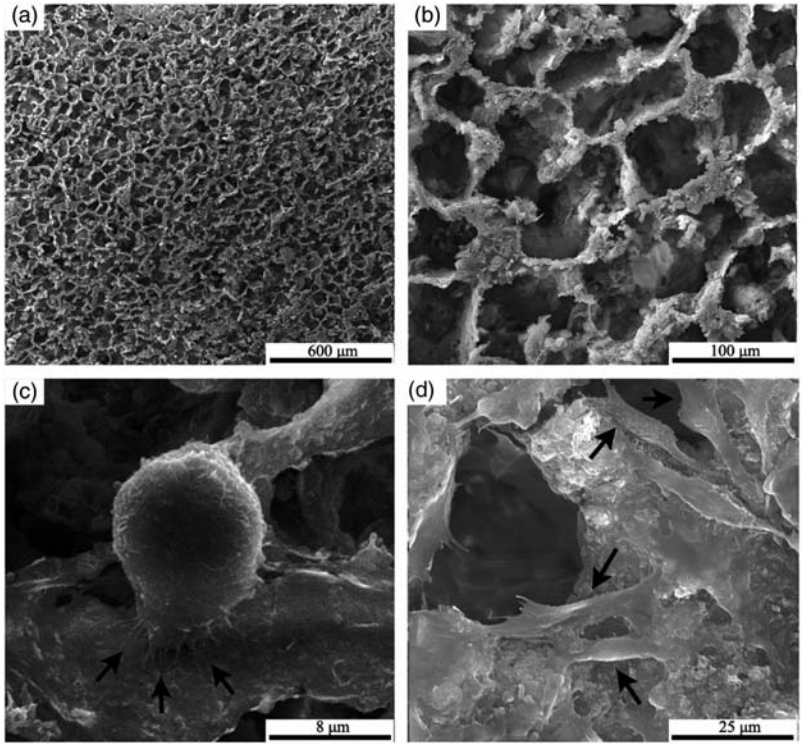

Figure 6. SEM observations of nHAC/PLA scaffolds and seeded BMP-2 transfected MSCs. (a) nHAC/PLA scaffolds; (b) magnified view of central area of (a); (c) 2 h after cell seeding, the arrows show the microspikes and extended filopodia that attached to the surface of the scaffolds; (d) 1 day after cell seeding, the arrows show the cells that attached to the pore wall of the scaffold and bridged over pores partially.

radius segments were seen in the defect sites after 8 weeks in all the Group A rabbits (Figure 7(a)). In contrast, the rabbits in control, Group B, had only a trace of mineralization in the defect site without reconnection between the two ends of the radius segments (Figure 7(c)). After 12 weeks, the defect site was restored of all defects in Group A, at least 90% of the defect site was filled with cancellous ossification and the medullary cavity partly recanalized (Figure 7(b)). Radiographic bone union was observed in Group B, although the bone density was much lower than that of Group A (Figure 7(d)). However, Group B at 12 weeks was much better than that of Group C, where the defect reconstructed with just scaffolding appeared radiolucent in most of the defect (Figure 7(e)). No radiographic evidence of bone

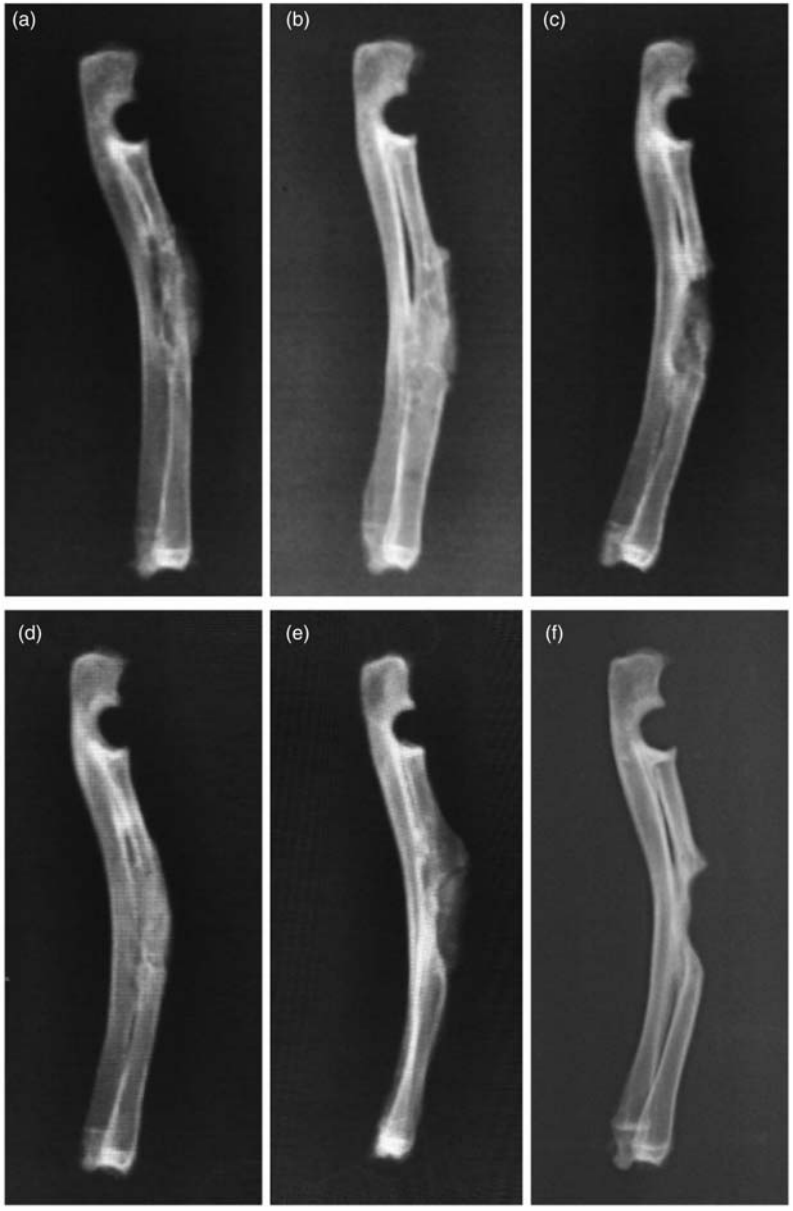

Figure 7. Representative radiograph of defects at 8 and 12 weeks post-operation. ((a) and (b)) Implantation of nHAC/PLA scaffolds combined with BMP-2 transfected MSCs (Group A) at 8 and 12 weeks; ((c) and (d)) implantation of nHAC/PLA scaffolds combined with mock-transfected MSCs (Group B) at 8 and 12 weeks; (e) implantation of just nHAC/PLA scaffolds (Group C) at 12 weeks; (f) implantation of nothing (Group D) at 12 weeks.

formation was present in the blank control group (Group D) after 12 weeks (Figure 7(f)).

Histological Examination

Histological examination of Group A showed large amounts of trabecular bone formation in the pores of the scaffolds after 8 weeks. The newly formed bone contained osteocyte-like cells embedded randomly in the bone matrix, and osteoblast-like cells in the lining on the surface of the developing bone (Figure 8(a)). After 12 weeks, a discrete amount of highly cellular bone marrow-like tissue that filled the space between the newly formed trabecular bone was observed. Interestingly, the residual scaffold was surrounded by marrow-like tissue in the medullary cavity (Figure 8(b)). In contrast, Group B showed lots of loose fibrous connective tissue in the pore space and a small amount of new bone generation in a few pores of the implant at 8 weeks (Figure 8(c)). With the implantation prolonged, more newly formed trabecular bone was observed in the presence of the active osteoblasts (Figure 8(d)). In Group C, connective tissue and inflammatory infiltration were present in superficial as well as inner pores and very few osteoid formations were observed both at 8 and 12 weeks post-operation (Figure 8(e) and (f)).

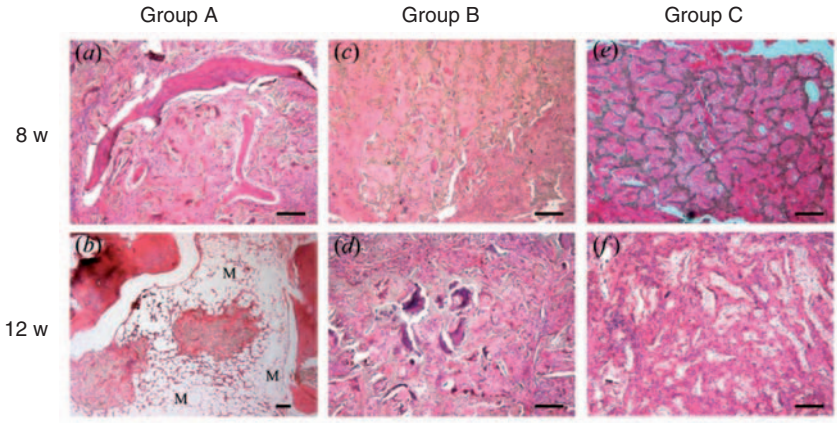

Figure 8. Representative sections of regenerating bones at 8 and 12 weeks post-implantation by HE staining (bar = 200 μm). ((a) and (b)) Implantation of nHAC/PLA scaffolds combined with BMP-2 transfected MSCs (Group A); ((c) and (d)) implantation of nHAC/PLA scaffolds combined with mock-transfected MSCs (Group B); ((e) and (f)) implantation of just nHAC/PLA scaffolds (Group C). In photo (b), M denotes bone marrow-like tissue.

DISCUSSION

Gene therapy represents an attractive and promising approach to bone regeneration. In this study, the osteogenesis of a novel, biodegradable 3D biomimetic construct was fabricated using BMP-2 transfected MSCs cultured in nHAC/PLA scaffold. *In vitro* and *in vivo* studies indicated that better osteogenesis was achieved and more advanced bone tissue was formed in contrast to other scaffolds.

Previous studies, evaluating the repair of bone defects using BMP protein, showed that this approach is effective in different animal models [35–37]. However, the BMP protein therapies are hampered by high manufacturing costs, undesirable side effects and lack of a good system to deliver proteins [38]. Therefore, BMP gene therapy is currently being developed to enhance bone regeneration by both *in vivo* and *in vitro*. Moreover, the protein produced endogenously by gene transfer has undergone authentic post-translational modification and, therefore, may show improved potency [22]. The safety and immunogenicity remain obstacles to the development of efficient gene therapy protocols [39].

Currently, MSCs are the most widely used cell source for bone tissue engineering [10,18]. In addition to their easy acquirement and high differentiation potential to osteoblasts, low immunogenicity also makes MSCs more suitable for bone tissue engineering [40].

A variety of viral vectors have been used in BMP-2 *in vitro* gene therapy to induce osteogenesis [18,20,41]. Although nonviral gene delivery system is less efficient than viral gene delivery, it has the advantages of unrestricted capacity for delivering gene, safety, and simplicity of use [42]. In this study of transfected MSCs with the pIRES2-EGFP-hBMP-2 gene using electroporation, the transfer efficiency reached $35.8 \pm 4.4\%$ under optimal conditions. To use gene delivery as a BMP-2 delivery strategy, long-term BMP-2 expression may be unnecessary for all stages of the fracture healing process. Recently, it was demonstrated that BMP-2 plays an important role, particularly, during the early stage of bone regeneration [43]. In support of this, Marsh et al. [44] reported that BMPs were key elements in the cascade of molecular events required for bone repair during fracture healing. Actually, a short-term expression of BMP-2 may not only be adequate to trigger the cascade of events leading to skeletal development and repair, but also prevent excessive ossification that potentially occurs after a long-term BMP-2 expression [42]. That plasmid-mediated BMP-2 gene transfer to MSCs led to healing of critical-sized bone defects in rabbits was corroborated by Park et al. [20], who used both plasmid

and adenovirus-mediated BMP-2 gene transfer to MSC-promoted healing of critical-sized bone defects in rats.

In tissue engineering, the choice of ideal material is crucial to tissue regeneration. Besides good compatibility, osteoconductivity, and biodegradability, scaffold for bone tissue regeneration should possess a 3D porous structure with porosity no less than 70% and pore size ranging from 50 to 900 μm [45,46]. nHAC/PLA, fabricated by biomimetic strategy, has a 3D structure with a porosity of about 75% and pore size of about 50–300 μm. Previous studies had reported that this material demonstrated adequate compatibility, superior osteoconduction, and biodegradability [29]. HA [47], collagen [48], or 3D environment [49,50] has the potential to promote stem cells' osteogenic differentiation independently. Therefore, it is conceivable that the 3D nHAC/PLA scaffolds, to some extent, are able to promote MSCs osteogenic differentiation.

In this *in vitro* study, the BMP-2 transfected MSCs had attached to the pore walls of the nHAC/PLA scaffold with some of their pseudopodia beginning to bridge over pores just 1 day after cell seeding. Thus, the 3D nHAC/PLA facilitated gene-modified MSC adhesion and proliferation on the scaffold. A critical-sized defect (CSD) *in vivo* is one that will not regenerate spontaneously during the term of an experiment. A 15 mm CSD in the radius of rabbit model has been shown to maintain its size for 4 months [45]. In this study, according to the histological and radiographic results, large amounts of mature bony callus had formed in the BMP-2 gene-modified MSCs/scaffold construct in 8 weeks. After 12 weeks, the regeneration of all defects exhibited complete healing.

CONCLUSIONS

Based on *in vitro* data, BMP-2 transfected MSCs enhanced attachment and growth in nHAC/PLA scaffolds. Subsequently, critical-sized segmental defects on the rabbit radius were evaluated *in vivo*. According to the histological and radiographic results, the BMP-2 transfected MSCs/nHAC/PLA construct enhanced and accelerated bone formation in the segmental defects compared to the control. This novel, biodegradable 3D BMP-2 transfected MSCs/nHAC/PLA construct could potentially be a candidate for bone tissue engineering.

ACKNOWLEDGMENTS

This study was supported in part by two National Natural Science Foundation of China (NNSFC, nos. 50830102 and 50573044), and the

Shandong Provincial Program of Science and Technology Development (no. 023130110).

REFERENCES

1. Khan, S.N., Cammisa Jr, F.P., Sandhu, H.S., Diwan, A.D., Girardi, F.P. and Lane, J.M. (2005). The Biology of Bone Grafting, *J. Am. Acad. Orthop. Surg.*, **13**: 77–86.
2. Pelissier, P., Boireau, P., Martin, D. and Baudet, J. (2003). Bone Reconstruction of the Lower Extremity: Complications and Outcomes, *Plast. Reconstr. Surg.*, **111**: 2223–2229.
3. Hill, N.M., Horne, J.G. and Devane, P.A. (1999). Donor Site Morbidity in the Iliac Crest Bone Graft, *Aust. N. Z. J. Surg.*, **69**: 726–728.
4. Younger, E.M. and Chapman, M.W. (1989). Morbidity at Bone Graft Donor Sites, *J. Orthop. Trauma*, **3**: 192–195.
5. Bauer, T.W. and Muschler, G.F. (2000). Bone Graft Materials. An Overview of the Basic Science, *Clin. Orthop. Relat. Res.*, **371**: 10–27.
6. Greenwald, A.S., Boden, S.D., Goldberg, V.M., Khan, Y., Laurencin, C.T. and Rosier, R.N. (2001). Bone-Graft Substitutes: Facts, Fictions, and Applications, *J. Bone Joint Surg. Am.*, **83-A**: 98–103.
7. Bauer, T.W. and Smith, S.T. (2002). Bioactive Materials in Orthopaedic Surgery: Overview and Regulatory Considerations, *Clin. Orthop. Relat. Res.*, **395**: 11–22.
8. Vacanti, C.A. and Bonassar, L.J. (1999). An Overview of Tissue Engineered Bone, *Clin. Orthop. Relat. Res.*, **367**: S375–S381.
9. Muschler, G.E., Nakamoto, C. and Griffith, L.G. (2004). Engineering Principles of Clinical Cell-Based Tissue Engineering, *J. Bone Joint Surg. Am.*, **86A**: 1541–1558.
10. Justesen, J., Stenderup, K. and Kassem, M.S. (2001). Mesenchymal Stem Cells. Potential Use in Cell and Gene Therapy of Bone Loss Caused by Aging and Osteoporosis, *Ugeskr Laeger*, **163**: 5491–5495.
11. Pelled, G., Turgeman, G., Aslan, H., Gazit, Z. and Gazit, D. (2002). Mesenchymal Stem Cells for Bone Gene Therapy and Tissue Engineering, *Curr. Pharm. Des.*, **8**: 1917–1928.
12. Gazit, D., Turgeman, G., Kelley, P., Wang, E., Jalenak, M., Zilberman, Y. et al. (1999). Engineered Pluripotent Mesenchymal Cells Integrate and Differentiate in Regenerating Bone: A Novel Cell-Mediated Gene Therapy, *J. Gene Med.*, **1**: 121–133.
13. Kimelman, N., Pelled, G., Gazit, Z. and Gazit, D. (2006). Applications of Gene Therapy and Adult Stem Cells in Bone Bioengineering, *Regen. Med.*, **1**: 549–561.
14. Franzen, A. and Heinegard, D. (1984). Extraction and Purification of Proteoglycans from Mature Bovine Bone, *Biochem. J.*, **224**: 47–58.

15. Cheng, H., Jiang, W., Phillips, F.M., Haydon, R.C., Peng, Y., Zhou, L. et al. (2003). Osteogenic Activity of the Fourteen Types of Human Bone Morphogenetic Proteins (BMPs), *J. Bone Joint Surg. Am.*, **85-A**: 1544–1552.
16. Ma, X., Wu, X., Hu, Y., Xiong, Z., Lv, R., Wang, J. et al. (2009). Intervertebral Spinal Fusion Using a RP-Based PLGA/TCP/Bbmp Biomimetic Grafting Material, *J. Bioact. Compat. Polym.*, **24**: 146–157.
17. Alden, T.D., Varady, P., Kallmes, D.F., Jane Jr, J.A. and Helm, G.A. (2002). Bone Morphogenetic Protein Gene Therapy, *Spine (Phila Pa 1976)*, **27**: S87–S93.
18. Partridge, K., Yang, X., Clarke, N.M., Okubo, Y., Bessho, K., Sebald, W. et al. (2002). Adenoviral BMP-2 Gene Transfer in Mesenchymal Stem Cells: In vitro and In vivo Bone Formation on Biodegradable Polymer Scaffolds, *Biochem. Biophys. Res. Commun.*, **292**: 144–152.
19. Chang, S.C., Chuang, H.L., Chen, Y.R., Chen, J.K., Chung, H.Y., Lu, Y.L. et al. (2003). Ex vivo Gene Therapy in Autologous Bone Marrow Stromal Stem Cells for Tissue-engineered Maxillofacial Bone Regeneration, *Gene Ther.*, **10**: 2013–2019.
20. Park, J., Ries, J., Gelse, K., Kloss, F., von der Mark, K., Wiltfang, J. et al. Bone Regeneration in Critical Size Defects by Cell-mediated BMP-2 Gene Transfer: A Comparison of Adenoviral Vectors and Liposomes, *Gene Ther.*, **10**: 1089–1098.
21. Wu, W., Zhang, Y., Li, H. and Wanshan, Z. (2009). Fabrication of Repairing Skull Bone Defects Based on the Rapid Prototyping, *J. Bioact. Compat. Polym.*, **24**: 125–136.
22. Guo, X., Zheng, Q., Yang, S., Shao, Z., Yuan, Q., Pan, Z. et al. (2006). Repair of Full-thickness Articular Cartilage Defects by Cultured Mesenchymal Stem Cells Transfected with the Transforming Growth Factor Beta1 Gene, *Biomed. Mater.*, **1**: 206–215.
23. Weber, M., Steinert, A., Jork, A., DimmLer, A., Thurmer, F., Schutze, N. et al. (2002). Formation of Cartilage Matrix Proteins by BMP-Transfected Murine Mesenchymal Stem Cells Encapsulated in a Novel Class of Alginates, *Biomaterials*, **23**: 2003–2013.
24. Guo, X., Zheng, Q., Kulbatski, I., Yuan, Q., Yang, S., Shao, Z. et al. (2006). Bone Regeneration with Active Angiogenesis by Basic Fibroblast Growth Factor Gene Transfected Mesenchymal Stem Cells Seeded on Porous Beta-TCP Ceramic Scaffolds, *Biomed. Mater.*, **1**: 93–99.
25. Kale, S., Biermann, S., Edwards, C., Tarnowski, C., Morris, M. and Long, M.W. (2000). Three-dimensional Cellular Development is Essential for Ex vivo Formation of Human Bone, *Nat. Biotechnol.*, **18**: 954–958.
26. Putnam, A.J. and Mooney, D.J. (1996). Tissue Engineering Using Synthetic Extracellular Matrices, *Nat. Med.*, **2**: 824–826.

27. Wang, Y., Kim, U.J., Blasioli, D.J., Kim, H.J. and Kaplan, D.L. (2005). In vitro Cartilage Tissue Engineering with 3D Porous Aqueous-Derived Silk Scaffolds and Mesenchymal Stem Cells, *Biomaterials*, **26**: 7082–7094.
28. Liao, S.S., Cui, F.Z., Zhang, W. and Feng, Q.L. (2004). Hierarchically Biomimetic Bone Scaffold Materials: Nano-HA/Collagen/PLA Composite, *J. Biomed. Mater. Res. B Appl. Biomater.*, **69B**: 158–165.
29. Xie, L.N., Wang, P., Cui, F.Z., Pan, J.L. and Sun, Z. (2010). The Effect of Platelet-Rich Plasma with Mineralized Collagen-Based Scaffold on Mandible Defect Repair in Rabbits, *J. Bioact. Compat. Polym.*, **24**: 543–559.
30. Zhou, D.S., Zhao, K.B., Li, Y., Cui, F.Z. and Lee, I.S. (2006). Repair of Segmental Defects with Nano-Hydroxyapatite/Collagen/PLA Composite Combined with Mesenchymal Stem Cells, *J. Bioact. Compat. Polym*., **21**: 373–384.
31. Zhang, C., Hu, Y.Y., Cui, F.Z., Zhang, S.M. and Ruan, D.K. (2006). A Study on a Tissue-Engineered Bone Using rhBMP-2 Induced Periosteal Cells with a Porous Nano-hydroxyapatite/Collagen/Poly(L-Lactic Acid) Scaffold, *Biomed. Mater.*, **1**: 56–62.
32. Zou, D., Zhou, D. and Wang, Y. (2006). Expression and Mechanism of cDNA of Human Bone Morphogenetic Protein 2 via Eukaryotic Expression Vector in Rabbit Mesenchymal Stem Cells, *Chin. J. Orthop. Trauma*, **8**: 148–152.
33. Zhang, X., Carpenter, D., Bokui, N., Soo, C., Miao, S., Truong, T. et al. (2003). Overexpression of Nell-1, a Craniosynostosis-associated Gene, Induces Apoptosis in Osteoblasts During Craniofacial Development, *J. Bone Miner. Res*., **18**: 2126–2134.
34. Cui, F., Li, Y. and Ge, J. (2007). Self-assembly of Mineralized Collagen Composites, *Mater. Sci. Eng. R Rep.*, **57**: 1–27.
35. Zhu, H., Wu, Q., Shentu, J., Wang, H., Hu, Y., Zhu, K. et al. (2005). Release Behavior and Biological Activity of Recombinant Human Bone Morphogenetic Protein-2 from Porous PLGA Scaffold, *J. Bioact. Compat. Polym*., **20**: 271–278.
36. Tuominen, T., Jamsa, T., Tuukkanen, J., Nieminen, P., Lindholm, T.C., Lindholm, T.S. et al. (2000). Native Bovine Bone Morphogenetic Protein Improves the Potential of Biocoral to Heal Segmental Canine Ulnar Defects, *Int. Orthop.*, **24**: 289–294.
37. Kokubo, S., Nozaki, K. and Takahashi, K. (2008). Recombinant Human Bone Morphogenetic Protein-2 as an Osteoinductive Biomaterial and a Biodegradable Carrier in a Rabbit Ulnar Defect Model, *J. Bioact. Compat. Polym.*, **23**: 348–366.
38. Li, R.H. and Wozney, J.M. (2001). Delivering on the Promise of Bone Morphogenetic Proteins, *Trends Biotechnol.*, **19**: 255–265.
39. Barbour, V. (2000). The Balance of Risk and Benefit in Gene-Therapy Trials, *Lancet*, **355**: 384.

40. Ozawa, K., Sato, K., Oh, I., Ozaki, K., Uchibori, R., Obara, Y. et al. (2008). Cell and Gene Therapy Using Mesenchymal Stem Cells (MSCs), *J. Autoimmun.*, **30**: 121–127.
41. Hsu, W.K., Sugiyama, O., Park, S.H., Conduah, A., Feeley, B.T., Liu, N.Q. et al. (2007). Lentiviral-Mediated BMP-2 Gene Transfer Enhances Healing of Segmental Femoral Defects in Rats, *Bone*, **40**: 931–938.
42. Attia, J., Boumédiène, K., Pujol, J.P., Valleton, J.M., Huet, E. and Nguyen, Q.T. (2009). Matrix Gene Expression in Dermal Fibroblasts Cultured on Hyaluronan-Coated Scaffolds, *J. Bioact. Compat. Polym.*, **24**: 329–349.
43. Southwood, L.L., Frisbie, D.D., Kawcak, C.E., Ghivizzani, S.C., Evans, C.H. and McIlwraith, C.W. (2004). Evaluation of Ad-BMP-2 for Enhancing Fracture Healing in an Infected Defect Fracture Rabbit Model, *J. Orthop. Res.*, **22**: 66–72.
44. Marsh, D.R. and Li, G. (1999). The Biology of Fracture Healing: Optimising Outcome, *Br. Med. Bull.*, **55**: 856–869.
45. Beskardes, B.I. and Gümüsderelioglu, M. (2009). Biomimetic Apatite-coated PCL Scaffolds: Effect of Surface Nanotopography on Cellular Functions, *J. Bioact. Compat. Polym.*, **24**: 507–524.
46. Li, H., Zheng, Q., Xiao, Y., Feng, J., Shi, Z. and Pan, Z. (2009). Rat Cartilage Repair Using Nanophase PLGA/HA Composite and Mesenchymal Stem Cells, *J. Bioact. Compat. Polym.*, **24**: 83–99.
47. Tsiridis, E., Ali, Z., Bhalla, A., Gamie, Z., Heliotis, M., Gurav, N. et al. (2009). In vitro Proliferation and Differentiation of Human Mesenchymal Stem Cells on Hydroxyapatite Versus Human Demineralised Bone Matrix with and without Osteogenic Protein-1, *Expert Opin. Biol. Ther.*, **9**: 9–19.
48. Kihara, T., Hirose, M., Oshima, A. and Ohgushi, H. (2006). Exogenous Type I Collagen Facilitates Osteogenic Differentiation and Acts as a Substrate for Mineralization of Rat Marrow Mesenchymal Stem Cells In Vitro, *Biochem. Biophys. Res. Commun.*, **341**: 1029–1035.
49. Mohr, J.C., de Pablo, J.J. and Palecek, S.P. (2006). 3-D Microwell Culture of Human Embryonic Stem Cells, *Biomaterials*, **27**: 6032–6042.
50. Machado, C.B., Ventura, J.M., Lemos, A.F., Ferreira, J.M., Leite, M.F. and Goes, A.M. (2007). 3D Chitosan–Gelatin–Chondroitin Porous Scaffold Improves Osteogenic Differentiation of Mesenchymal Stem Cells, *Biomed. Mater.*, **2**: 124–131.